Potential of prompt γ-ray emission studies in fast-neutron induced fission: a first step

L. Qi, C. Schmitt, M. Lebois, A. Oberstedt, S. Oberstedt, J.N. Wilson, A. Al-Adili, A. Chatillon, D. Choudhury, A. Gatera, et al.

Eur. Phys. J. A (2020) 56:98
https://doi.org/10.1140/epja/s10050-020-00108-w

THE EUROPEAN PHYSICAL JOURNAL A

Regular Article - Experimental Physics

Potential of prompt γ-ray emission studies in fast-neutron induced fission: a first step

L. Qi[1], C. Schmitt[2,a], M. Lebois[1], A. Oberstedt[3], S. Oberstedt[4], J. N. Wilson[1], A. Al-Adili[5], A. Chatillon[6], D. Choudhury[3], A. Gatera[4], G. Georgiev[7], A. Göök[4], B. Laurent[6], A. Maj[8], I. Matea[1], S. J. Rose[9], B. Wasilewska[8], F. Zeiser[9]

[1] Institut de Physique Nucleaire, Rue Georges Clemenceau, Univ. Paris-Sud, 91406 Orsay Cedex, France
[2] Institut Pluridisciplinaire Hubert Curien, 23 Rue du Loess, B.P. 28, 67037 Strasbourg Cedex 2, France
[3] Extreme Light Infrastructure-Nuclear Physics (ELI-NP)/Horia Hulubei National Institute for Physics and Nuclear Engineering (IFIN-HH), 077125 Bucharest-Magurele, Romania
[4] European Commission, Joint Research Centre, Directorate G for Nuclear Safety and Security, Unit G.2, 2440 Geel, Belgium
[5] Department of Physics and Astronomy, Uppsala University, Box 516, 751 20 Uppsala, Sweden
[6] CEA, DAM, DIF, 91297 Arpajon, France
[7] CSNSM, CNRS-IN2P3, Univ. Paris-Sud, 91406 Orsay Cedex, France
[8] Institute of Nuclear Physics Polish Academy of Sciences, 31-342 Krakow, Poland
[9] Department of Physics, University of Oslo, P.O. Box 1048, Blindern, 0316 Oslo, Norway

Received: 13 December 2019 / Accepted: 27 February 2020 / Published online: 25 March 2020

Communicated by Jose Benlliure

Abstract Prompt γ-ray spectra emitted in fast-neutron induced fission of ^{239}Pu have been recently measured by using the LICORNE directional neutron source at E_n = 1.8 MeV. The results are used in parallel with the measurements of fast-neutron induced fission of ^{238}U and spontaneous fission of ^{252}Cf to assess the potential of such reactions and observables, in contributing to the understanding of fission. The γ-ray spectra were measured and analyzed under similar conditions, allowing a consistent and robust comparison between the three systems. They are further compared to Monte–Carlo simulations based on two widely-used semi-empirical codes, FREYA and GEF. Differences in the low and high energy portions of the spectrum are interpreted based on simple arguments involving nuclear structure and evaporation effects. The significance and potential of experimental campaigns of this kind, as well as current limitations, are highlighted, together with straightforward but mandatory extensions.

1 Introduction

It is well-established that nuclear fission constitutes a particularly interesting phenomenon for both fundamental research and applied science (see Refs. [1,2] for recent reviews). Understanding the evolution of the process from threshold up to moderate excitation energy is, in particular, a challenging problem, as it raises the question of the respective role of nuclear structure in the nascent fragments and nuclear dynamics. An accurate knowledge around and above threshold is also crucial for applications.

So far, models and codes in the domain focus on spontaneous and thermal-neutron-induced fission, for which most numerous and accurate information exists. However, their ability to explain consistently the available data is still limited. In particular, describing neutron and γ-ray emission properties *simultaneously* remains a problem in most cases (see e.g. Refs. [3–9]). Part of the difficulty comes from the intricate interplay of the influence of emitter mass A, charge Z, excitation energy E^*, and angular momentum L, in determining the neutron and γ-ray observables. These dependences induce natural correlations between fission neutrons and γ rays [10,11]. For a single fissioning system, a wide population (a few hundreds) of primary fragments is generated in the (A, Z, E^*, L) space. Varying separately these four variables, or disentangling them, is impossible in practice, what magnifies the complexity of correlations in the integral spectrum. Focus during the last decades has been on the description of neutrons, while γ rays received little attention. However, the understanding of one observable cannot occur in isolation to the other. Furthermore, γ rays on their own are important for understanding specific aspects of the fission process. Fission γ-rays are a key issue in nuclear

[a] e-mail: christelle.schmitt@iphc.cnrs.fr (corresponding author)

reactors. The international OECD/NEA agency considers as priority [12] the need to improve the existing simulations of heating caused by γ rays. Recent studies [13–16] excluded thermal-neutron-induced fission as the cause of the underestimation of γ-ray heating by current calculations. Fast-neutron induced fission may be the cause. A crisp review on the history of prompt fission γ-ray studies, status, open questions and perspectives, can be found in Ref. [17].

The aim of the present work is to contribute to the ongoing worldwide investigation by exploiting the results of a recent experimental campaign [18–20] on fast-neutron induced fission of ^{238}U and ^{239}Pu, including also spontaneous fission of ^{252}Cf, at the ALTO/LICORNE facility [21], IPN Orsay, France. The results for n+^{239}Pu are presented for the first time. The experimental data are compared to calculations obtained with two semi-empirical codes widely-distributed in the field, with the goal to investigate to which extent the measurements are capable of evidencing differences between the three systems, and correlate it with the underlying physics. The calculations are used to offer an explanation for some experimental observations, whereas some other remain un-explained, as it appears impossible to discriminate between different physics scenarios. Similar comparisons can be found in literature (representative papers are quoted in this paper). The focus was mainly on testing models with benchmark data, and eventually address some physics case. In this context, the present work is instead intended to study in a dedicated and detailed manner to which level of confidence and accuracy this is possible. It shows which specific physics question can, or not, be reliably accessed with certain observables measured in certain conditions. The work sheds light on the influence of critical limitations of current experiments, as well as it points to some required developments.

2 Measurements

2.1 Setup

The Prompt-Fission γ-ray spectrum (PFGS) from fast-neutron induced fission of ^{239}Pu was measured at the ALTO/LICORNE facility, IPN Orsay, France. The reaction p(^{7}Li, n)^{7}Be was used to generate a quasi-monoenergetic kinematically focused neutron beam of energy $E_n = 1.8$ MeV. To select fission events, a specifically-designed fission chamber was constructed at JRC-Geel, containing the ^{239}Pu sample [18,20]. The purity and total mass of the ^{239}Pu sample was 99.97% and 3.519 mg, respectively. The charge signals of the fission chamber permitted to discriminate fission fragments from α particles. A particularly efficient method based pulse shape discrimination was developed, and permitted to recover 7% of true fission events, which pulse height overlaped with the α bump. Details and spectra have been reported in Ref. [20]. The total number of fission events collected amounts to 5.5×10^6. Prompt fission γ-rays were measured using two types of fast scintillators: 6 individual $LaBr_3$(Ce) (cylindrical $2'' \times 2''$ and $3'' \times 3''$ crystals) detectors located at distances between 34 and 45cm from the target, and the first cluster of the PARIS array [22] encompassing 9 new type of $LaBr_3$(Ce)-NaI(Tl) phoswich cells (cubic $2'' \times 2'' \times 2''$ $LaBr_3$(Ce) crystals followed with rectangular $2'' \times 2'' \times 6''$ NaI(Tl) crystals) located at 40cm. The measured energy resolution amounted to 3% and 5% at E_γ = 661 keV, respectively, for the $LaBr_3$(Ce) detectors and PARIS phoswiches. The efficiency at 1.33MeV was measured to be 0.029% for the smallest $LaBr_3$(Ce) detectors at closest distance, 0.036% for a PARIS phoswich, and 0.32% for the cluster [18]. The overall time resolution of the set-up (dominated by the fission chamber) had a Full Width at Half Maximum (FWHM) of $\approx$ 2 ns. Prompt photons were selected by setting a $\pm$ 3 ns wide time window around the γ-ray peak in the time-of-flight spectrum of each detector. The experimental threshold was tuned around a few tens of keV, such that it can be set sharp at 100 keV in further analysis. Standard and reaction γ-ray sources, with energies up to 9 MeV, were used for calibration and efficiency determination. We refer to Ref. [20] for further details.

The response function of each detector was obtained from an elaborate simulation of the entire set-up, which was validated by the source data [19]. The measured γ-ray spectra were unfolded from the corresponding response, and that result can be directly compared to model calculations. The average γ-ray multiplicity M_γ and total energy released by photon radiation $E_{\gamma,tot}$ can also be extracted from the unfolded PFGS as follows: M_γ is determined as the integral of the unfolded spectrum, and $E_{\gamma,tot}$ is obtained from the sum over the product of the spectral yields for each bin in the unfolded spectrum and its energy (*viz.* first moment of the distribution). Finally, the average energy per photon is derived according to $\epsilon_\gamma = E_{\gamma,tot}/M_\gamma$.

The measurements of fast-neutron induced fission of ^{238}U and spontaneous fission of ^{252}Cf were conducted during the same campaign, under the same conditions with the same setup, and analyzed in a similar way [19].

2.2 Experimental results

The mean characteristics of the PFGS for the three reactions discussed in this work are summarized in Table 1, including the average γ-ray multiplicity M_γ, total energy released by photons $E_{\gamma,tot}$, and average energy per photon ϵ_γ. The last two columns of Table 1 refer to set-up-dependent parameters. The energy ΔE and time Δt ranges refer to the gates applied to the data in order to define a detected γ-ray as prompt.

Table 1 Characteristics of the PFGS. Experimental results are shown together with the FREYA and GEF calculations. See the text

		M_γ (/fission)	$E_{\gamma,tot}$ (MeV)	ϵ_γ (MeV)	Ref.	Δt (ns)	ΔE (MeV)
^{252}Cf(sf)	Expt.	8.35 ± 0.20	6.64 ± 0.21	0.80 ± 0.02	[19]	5	0.1–6.0
	Expt.	8.30 ± 0.09	6.64 ± 0.10	0.80 ± 0.01	[23]	5	0.1–6.0
	Expt.	8.14 ± 0.40	7.65 ± 0.55	0.94 ± 0.05	[24]	10	0.15–10
	Expt.	8.75	8.52	–	[25]	8	Not specified
	GEF	7.17	6.52	0.91	–	–	0.1–6.0
	FREYA	8.31	7.10	0.85	–	1.5	0.1–6.0
n (E_n=1.9MeV)+^{238}U	Expt.	6.54 ± 0.19	5.25 ± 0.20	0.80 ± 0.04	[19]	5	0.1–6.0
	GEF	6.24	5.84	0.94	–	–	0.1–6.0
	FREYA	7.23	6.18	0.85	–	1.5	0.1–6.0
n (E_n=1.8MeV)+^{239}Pu	Expt.	7.23 ± 0.37	6.71 ± 0.37	0.91 ± 0.04	–	6	0.1–7.0
	GEF	6.72	6.76	1.00	–	–	0.1–7.0
	FREYA	7.38	7.06	0.96	–	1.5	0.1–7.0

The results for ^{239}Pu(n,f) at E_n = 1.8 MeV are presented for the first time (with some preliminary data shown in Ref. [20]). Its PFGS is displayed in Fig. 1 separately for the $LaBr_3$(Ce) detectors and the PARIS phoswiches. Fast-neutron induced fission of ^{238}U and spontaneous fission of ^{252}Cf from Refs. [18,19] are additionally selected in the discussion of this work to investigate the potential of PFGS for learning about fission. The considered set of measurements is relevant for several reasons. (i) The LICORNE campaign uses quasi-monoenergetic fast neutrons, which permit the population of the primary fragment (A, Z, E^*, L) phase-space in a different way from thermal-neutron-induced fission. Mapping the variable landscape is useful to unravel intricate dependences and correlations. (ii) The beam energy employed corresponds to initial excitation energies in the fissioning system still below neutron threshold, thus avoiding the complexity which multi-chance fission implies at higher bombarding energies. (iii) All three systems are measured and analyzed under identical conditions. The comparison between them is, therefore, robust, independent of systematics errors, which can sometimes complicate the comparison of results collected at different facilities or set-ups. (iv) The prompt fission γ-ray spectrum observable is collected with good efficiency and resolution over the wide dynamical range which fission γ rays can span. (v) Finally, the measurements by Qi et al. [18–20] contribute to the database required to resolve the problem of heat calculations in reactors, and namely for the n+^{238}U, ^{239}Pu reactions that are crucial in the context of Generator IV reactor concepts [17].

The mean γ-ray properties extracted from other measurements are also shown in the table. They are consistent with each other. The discrepancy noticed with the DANCE data [24,25] for ^{252}Cf was ascribed to detection inefficiency in the low-energy region due to absorption effects [26]. Though, we note also that the energy range, time window, and unfolding procedure are different as compared to the other presented measurements. Hence, it is difficult to unambiguously determine the reason for the difference.

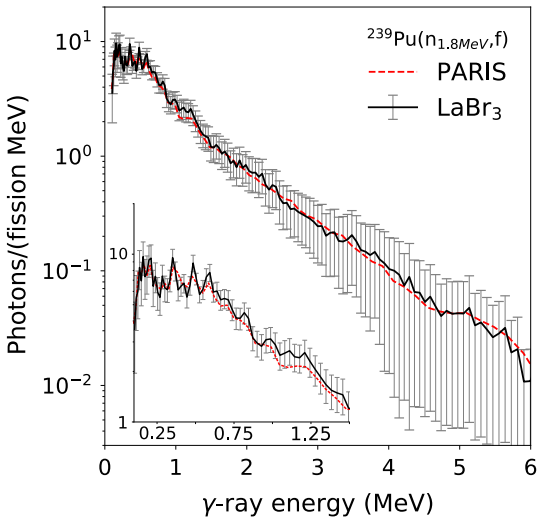

Fig. 1 Experimental PFGS for fast-neutron induced fission of ^{239}Pu for the $LaBr_3$(Ce) detectors (full black line) and the PARIS phoswiches (dashed red line). The inset shows the low-energy region. Error bars are shown for the $LaBr_3$(Ce) detectors, only, for legibility. They are similar for the PARIS phoswiches

The experimental PFGS of n+^{239}Pu, as well as n+^{238}U and ^{252}Cf(sf) [19], are overlaid in Fig. 2. Error bars are not shown for legibility reasons; they can be appreciated from e.g. Fig. 5. The upper panel in Fig. 2 shows the entire spectrum measured up to E_γ = 6 MeV, and the bottom one restricts to the low-energy region. Structures are clearly visible below $E_\gamma \approx 1$ MeV, while a smooth exponential fall-off is observed at higher energy. The structures at low energy are determined by the discrete transitions between low-lying excited states in the last stage of the fission-fragment de-excitation down

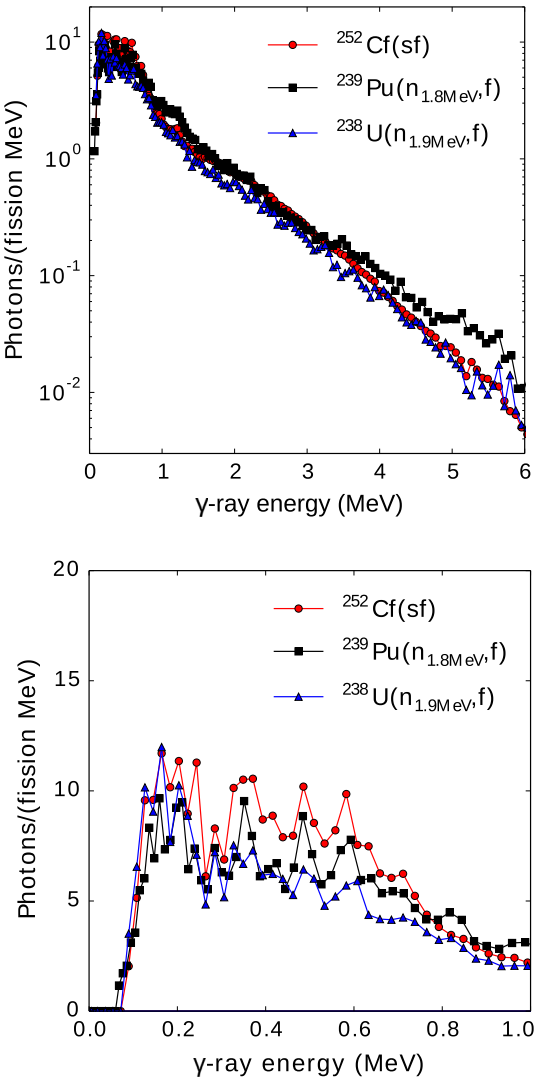

Fig. 2 Experimental PFGS [19,20] for spontaneous fission of ^{252}Cf and fast-neutron induced fission of ^{238}U and ^{239}Pu. The upper panel shows the entire measured spectrum, while the lower panel zooms the lower energy range

to the yrast line (or to an isomeric state). They do not appear as sharp peaks due to the combined effect of Doppler broadening, intrinsic detector resolution and absence of selectivity on fragment mass. These points will be discussed further below. The exponential decrease in the high-energy region is due to statistical emission which is largely dominated by the giant dipole resonance (GDR) built on excited states. The current data spectrum suffers from limited statistics and does not extend far enough in the E_γ range of the GDR peak, but the "low-energy" tail of the latter [27] impacts the highest-energy region accessible to the present experiments.

The comparison of the measured pattern at low E_γ shows that, while the intensity of the peaks decreases pretty fast between E_γ = 0.15 and 0.80 MeV for n+^{238}U, it remains rather constant over that range for ^{252}Cf; the behavior is intermediate for n+^{239}Pu. This difference between the three reactions is imputed on the different fragment (A, Z) populations. Since the heavy fragments are similar [1], namely for the n+^{239}Pu,^{238}U reactions, the difference observed in the PFGS may be ascribed to the light fragments. It is interesting to note that a very similar pattern is observed for the PFGS for spontaneous fission of ^{252}Cf as compared to those of thermal-neutron-induced fission of ^{235}U and ^{239}Pu [11].

The comparison of the experimental PFGS in the high-energy region suggests a harder spectrum for n+^{239}Pu. We quantified this difference by performing a fit to the PFGS between E_γ = 3 and 6 MeV with an exponentially decreasing function was done: The slope parameter was found to amount to 1.24, 0.97 and 1.20 MeV^{-2}, for ^{252}Cf, n+^{239}Pu, and n+^{235}U, respectively; that is, definitively smaller for n+^{239}Pu (the uncertainty on the extracted slopes is below 4%). Again the comparison of ^{252}Cf and thermal neutron-induced fission of ^{235}U and ^{239}Pu suggest a similar trend [11], although less pronounced.

3 Theoretical modeling

3.1 Calculation framework

Modeling fission remains a challenge for nuclear theory [2,28]. While qualitative description can be achieved by fundamental models, quantitative description is missing in most cases. Over the last several years, huge work was invested in the development of phenomenological and (semi-)empirical codes (see Refs. [3–8,10,29,30] and therein). These are computationally fast and flexible, as required for efficient implementation in general-purpose transport simulations modeling the interaction of radiation with almost everything (see e.g. Refs. [11,32–34]). Although predictive power is a major goal, these codes can also be useful to get insight into the underlying physics [35].

In the present work, calculations were performed with the two semi-empirical codes, FREYA [29] and GEF [10], which generate complete fission events, providing the full kinematic information on the two product fragments, the emitted neutrons and photons. The Monte-Carlo approach is adopted, permitting to naturally preserve correlations. Each code has its own specificities. The features of the codes, and their differences, which are most important for the present concern, are emphasized below.

FREYA is mainly dedicated to the modeling of the fragments de-excitation. It relies on the availability of "external" fragment yields (or reliable estimates) [31]. On the other hand, the de-excitation of the primary fragments formed at scission is thoroughly calculated. The fragments de-excite first by neutron evaporation. Once this is energetically forbidden, emission of statistical γ-rays starts, until the yrast line

(or a long-lived isomeric state) is reached. Noteworthy in our context is the recent implementation in the code of the RIPL3 data base for simulating the end of the decay cascade consisting of characteristic discrete γ-rays. In contrast to FREYA, in GEF the fragment yields are internally computed, based on a powerful semi-empirical modeling. In addition, the competition between neutron evaporation and emission of statistical γ-rays is accounted for. However, the yrast line is not taken from evaluation. Instead, the discrete excited levels characteristic of a nucleus are given by an analytical parameterization. Besides the aforementioned aspects, FREYA and GEF also differ regarding the generation and sharing of excitation energy and angular momentum between the two fragments at scission. The versions of the codes considered in this work are, respectively, the release v2.0.3 for FREYA [29], and GEF2016/V1.2 for GEF [10].

We note that the goal of the present work is *not* to put FREYA and GEF in competition. Similarly, we did not attempt to adjust parameters to specific reactions. Rather, the aim is to investigate the physics potential behind current experimental data with two different, well-established and representative codes in the field. In addition, FREYA and GEF are freely available, and widely used by the community. Practitioner users can thus evaluate what one shall expect when trying to interpret certain data with these tools. Several comparisons between fragment de-excitation codes like FREYA already exist [11,36,37], including parameter variation studies. Comparisons with GEF, which has its own fragment yield formalism, are scarce [38].

3.2 Calculation results

In the calculations, a number of 10^5 events were run for each reaction. Although this work focuses on prompt γ rays, we note that both the used codes give a reasonable description of other fission (fragment and neutron) properties for spontaneous fission of ^{252}Cf and thermal-induced fission of ^{235}U and ^{239}Pu [10,29].

The mean properties of the calculated PFGS are summarized in Table 1, in comparison with the experimental measurements. The γ-ray energy range ΔE and the time window Δt have a critical influence in the comparison between measured and calculated fission γ-ray properties [29,39]. As for the present study, the energy threshold with which the calculations were filtered is identical to the experimental one (100 keV). Regarding time window, the situation is somehow different. The parameter which governs time gating in FREYA is expressed in terms of the longest possible half-life t_{max} of an excited state so that its decay-out is recorded. It is set equal to the width of the experimental time window Δt, although it does not imply such a sharp gating. In GEF there is no explicit time gating: All transitions are recorded until an isomeric state, as tabulated in JEFF3.1.1, is reached along the decay cascade. According to our simulations [18] and detailed independent investigations [29,39] on the influence of the set-up-dependent ΔE and Δt parameters, discrepancies of the order of 5–10% can be reached between experiment and predictions for M_γ and $E_{\gamma,tot}$. Considering the experimental error bars, the complexity of a proper account of energy and time detection limit effects, and the robustness of unfolding procedures [19], the description of the mean PFGS characteristics by FREYA and GEF is estimated reasonable, and validates their use for the purpose of the present work. Furthermore, the codes have their own limited accuracy, due to the uncertainty of some parameters. According to the literature on FREYA and GEF, we estimate that, for the observables of this work, the calculated uncertainty is 5-10%. We note that best agreement between experiment and calculations in Table 1 is achieved by FREYA for ^{252}Cf (the default version of the code was tuned on this specific system, see also discussion in Ref. [29]).

The results of the FREYA calculations for the PFGS are presented in Fig. 3. They account for both the Doppler broadening and detector resolution. The GEF results are qualitatively the same. Contrary to the observation drawn from the measurements, the pattern exhibited by the calculated PFGS in the low-energy region is very similar for the three reactions, with the peak intensity steadily decreasing for $E_\gamma \in$ [0.15–0.80] MeV, independent of the fissioning system. That is, the singularity noticed in experiment for ^{252}Cf, with a nearly constant intensity at low energy, is not reproduced. The upper panel of Fig. 3 show that, unsurprisingly, the calculated spectra fall off exponentially above $E_\gamma \approx 2$ MeV; but most remarkable is that the calculations describe consistently the difference in hardness of the PFGS for the three systems: The n+^{239}Pu spectrum is unanimously harder. We emphasize that, thanks to the fact that all systems were measured in similar conditions, this difference can be firmly established, and it confirms what could so far only be considered as a prediction by the calculations. A discussion on the origin of the differences in the low-energy structures and high-energy hardness is proposed in Sects. 4.1 and 4.2, respectively.

4 Discussion

Prompt γ rays constitute a rich source of information in nuclear physics in general. The discrete γ rays emitted below the particle threshold are characteristic of a nucleus and constitute the best observable of its nuclear structure. Along the decay of excited and/or rotating nuclei, γ rays permit the probe of nuclear properties, among which the level-density in the continuum, and angular-momentum-driven effects. In heavy systems, γ-ray emission is in general in competition with neutron evaporation. Neutrons exhaust most of the excitation energy, while γ rays carry off most of the angular

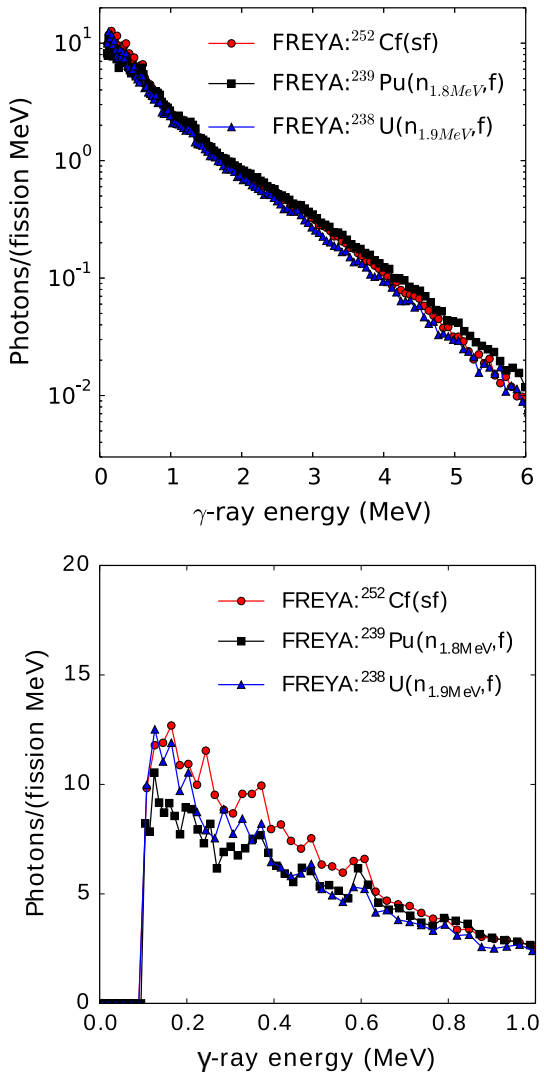

Fig. 3 Identical to Fig. 2 but as obtained from the FREYA calculations

momentum; both cooling processes are, therefore, necessarily correlated. For the specific case of a nuclear fission reaction, the aforementioned inter-dependences imply that the properties of prompt fission γ rays are a priori sensitive to the energetics of fission (namely the sharing of excitation energy between the two fragments, see e.g. Ref. [40]), to the generation and partition of angular momentum at scission [41], and finally, to the secondary fragment yields and properties [42,43].

4.1 Insight into the low-energy structures

As observed above, the calculations do not reproduce the singularity of ^{252}Cf in the low E_γ range. The comparison between the fission-fragment mass distributions for the three systems at low excitation energy [1] permits to highlight the fragment mass region which is intensively produced in ^{252}Cf fission, and not in the other two systems. Based on this, the deficiency of the calculated PFGS to explain the ^{252}Cf singularity is tentatively ascribed to the current spectroscopic knowledge of nuclei in the $A = 110-120$ range which would still not be that good.

The low-energy range of the PFGS exhibits rather broad peaks, rather than sharp lines as produced by the physics. In order to investigate the significance of such a measurement, we propose first to see how these broad peaks are produced, taking FREYA calculations as an example (GEF leads to the same). Since the fragment velocity vector is not available in the measurements by Qi et al. [18,19], Doppler effects cannot be corrected for. The corresponding boost is automatically taken into account by the FREYA software, and its influence is illustrated by the red spectrum in Fig. 4, which corresponds to the contribution of Xe isotopes to the low-energy part of the PFGS for the example of fast-neutron induced fission of ^{238}U. The different peaks are due to the population of various Xe masses, and with different intensities. The physical discrete lines are broadened by the Doppler effect, which amounts to about 3% in this case. The population of numerous Xe isotopes (around 10 with measurable intensity), and their close-lying lines, lead to the development of shoulders for some peaks, as well as the presence of a background. Adding the Sr isotopes, populated as the partners of Xe, gives rise to the blue spectrum. The pattern gets more and more dense, and a natural bunching of the Doppler-broadened lines occurs. Noteworthy also is the substantial increase of the background, and thus the decrease of the peak-to-valley ratio already for a single pair of fragment elements. In the lower panel, the influence of the absence of fragment selectivity is illustrated: The black spectrum is the superposition of the transitions from all fragments (around 300), what increases dramatically the effect of bunching of lines as well as the background. Finally, the detector resolution (around 3% at $E_\gamma = 0.662$ MeV) is included, leading to the red spectrum where structures are further smeared out. This exercise suggests that the low-energy part of the PFGS as available from the experiments of this work is not sensitive to the post-neutron fragment population in detail. The implications of this limited sensitivity is discussed below.

Since neutrons exhaust most of the excitation energy stored in the primary fragments, they are more direct signatures of E^* sharing at scission [3–6,44]. Emission of γ rays essentially sets in around the neutron separation energy. Hence, the PFGS is expected less sensitive to E^* sharing, and various calculations confirm this [45,46]. Nevertheless, due to the strong dependence of neutrons on E^* sharing, and the established correlations between neutrons and γ rays (see Ref. [38] and therein), the PFGS can be affected to some extent by the E^* sharing mechanism, too. The dependence is indirect, being due to the dependence of the secondary (A, Z) fragment population on excitation energy partition-

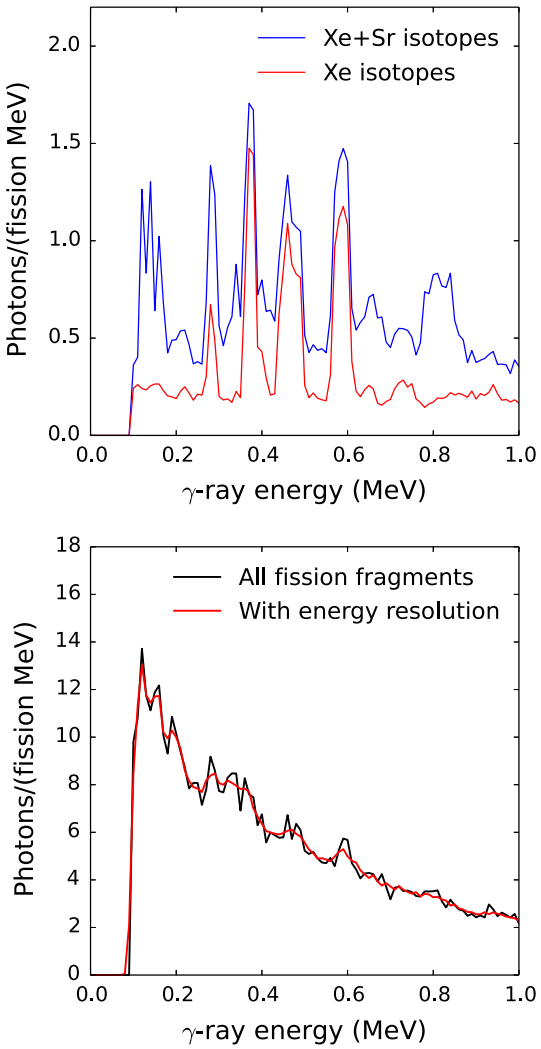

Fig. 4 Upper panel: Low-energy part of the PFGS as calculated by FREYA for n+^{238}U restricted to the contributions from Xe fragments (red), and to the contributions from Xe-Sr pairs (blue). Only Doppler effects are accounted for. Lower panel: PFGS including all fragments and accounting for Doppler effects (black), as well as intrinsic detector resolution (red)

ing. Our study, therefore, shows that the low-energy region of the PFGS from the measurements of Qi et al. [19,20] is not sensitive to E^* sharing at scission for a *given* system. However, a variant of the experiment [17], supplemented by mass selectivity, clearly establishes the dependence of the low-energy structure pattern on fragment population. That is, when exploited at maximum of its potential, measurements using the same approach and technology can be useful to study the sharing of the excitation energy between the two fragment. Mass selectivity is more critical than resolution in this case.

Although sensitivity to the detailed population for a given system is out of reach, the structures clearly depend on the fissioning system. That is, the experiment may be exploited still to study E^* sharing at scission by considering different systems at a time. In Fig. 5, for fast-neutron induced fission of ^{238}U as an example, the experimental PFGS is compared with FREYA and GEF calculations. The lower panel shows that the positions of the peaks calculated with FREYA match better the experimental ones than GEF does, although there are still differences in terms of intensity. The major difference between FREYA and GEF, and which impacts the low-E$_\gamma$ structures, is the modeling of the discrete excited states. As specified in Sect. 3.1, the latter are taken from the RIPL3 data base for FREYA, while they are based on a fully analytical formalism in GEF, which, in terms of accuracy, can of course, not compete with RIPL3. Therefore, the present study demonstrates that the experiments used here are sensitive to the accuracy in the modeling of discrete excited states. It also confirms that this type of experiments may be exploited to some extent in the context of nuclear structure [17], namely when some mass selectivity and Doppler effects correction are available [47].

4.2 Insight into the high-energy region

The high-energy part is less sensitive to uncorrected Doppler effects and intrinsic detector resolution, due to the very low density of discrete lines above 2 MeV. Statistical γ-ray emission (mainly from the GDR) depends on emitter temperature, nuclear level density and photon strength function [48,49]. Except in the vicinity of closed shells, their properties vary in a smooth way with emitter A and Z. For a *given* fissioning system, a modification of the fragment population within a realistic range is then expected to affect only weakly the high energy tail of the PFGS. We have confirmed this conjecture by comparing the high-energy part of the spectrum obtained from FREYA when using as input two different primary fragment populations, which calculations we mentioned already in Sect. 4.1. Both populations exhibit a very similar exponential fall-off at high E$_\gamma$. However, while this is true for a *given* system, it is obviously not, when comparing *different* fissioning systems, which can be characterized by more dramatic changes in fragment population, and hence temperature, level density, photon strength and GDR properties. In other words, similarly to the comment made for the low-energy side, the comparison of various systems may be exploited to study E^* sharing at scission to some extent. This endeavor is out of the scope of this manuscript. A recent work by Chyzh et al. [50] based on Pu fission with different entrance channels may tentatively be interpreted in a similar way.

As seen from the upper panel of Fig. 5 the calculations describe pretty well the n+^{238}U measurement above 2 MeV (the GEF spectrum is slightly too rounded – a feature already noticed in Ref. [10] and which is still un-explained). A similar achievement is observed for the other two systems [18]. Although the GDR peak of typical fission frag-

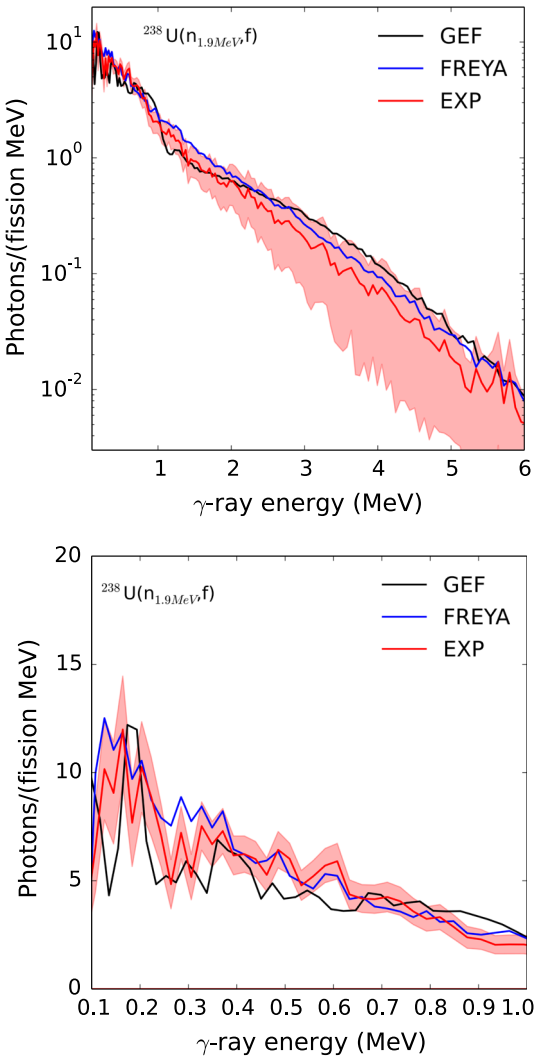

Fig. 5 Comparison between the experimental (red lines) and calculated (blue and black lines for FREYA and GEF, respectively) PFGS [19] for n+^{238}U. The upper panel shows the full E_γ range, while the lower panel restricts to $E_\gamma \in [0–1]$ MeV. Shadowed red bands give the range of the experimental error bars

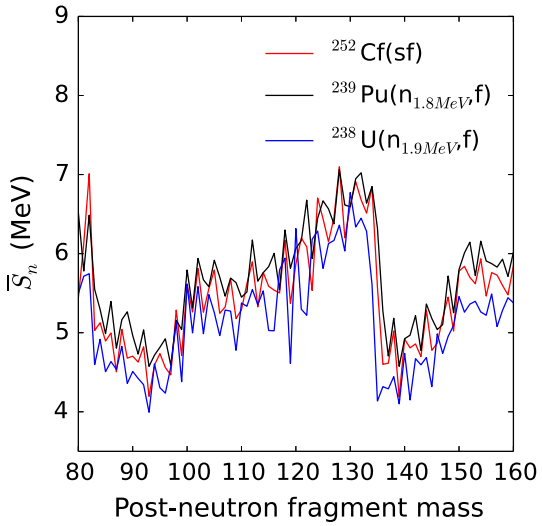

Fig. 6 Average neutron separation energies as a function of secondary-fragment mass number as obtained with FREYA for the three systems considered in this work

ments is located around 15 MeV, Vogt et al. [29] demonstrated the huge impact of the tail of the GDR down to $E_\gamma \approx$ 3 MeV. In other words, measurements of the type as those by Qi et al. [19] are presumably sensitive to the properties of the GDR built on excited states, and namely to its width, which dependence on temperature is controversial [51].

As discussed above, an important observation of the measurements is the harder spectrum for fast-neutron induced fission of ^{239}Pu as compared to spontaneous fission of ^{252}Cf and fast-neutron induced fission of ^{238}U. As noted too, calculations consistently describe the dependence of the PFGS hardness on the system, see Fig. 3 (upper panel). According to the good description of the measured exponential fall-off by the calculations, an interpretation for the "hierarchy" in PFGS hardness is proposed in the following, based on these calculations.

Since γ-ray emission sets efficiently in at the neutron-emission threshold, the excitation energy of the fission product at the end of the neutron cascade is essentially given by the neutron separation energy S_n [18,29]. The evolution of the empirical S_n value [52] as function of the secondary fragment mass calculated with FREYA (after averaging over Z) is displayed in Fig. 6 for the three reactions studied in this work. A very similar picture is obtained when FREYA is replaced with GEF. Fast-neutron induced fission of ^{238}U populates on the average more neutron-rich fragments as compared to the other two systems, being therefore characterized by smaller secondary-fragment neutron separation energies. On the average the temperatures after neutron evaporation are thus lower, and the PFGS is expected to be the least hard. The separation energies involved in the ^{252}Cf and n+^{239}Pu systems are larger. At the same time, the weight of the S1 fission mode, which leads to fragments in the vicinity of ^{132}Sn is much larger for n+^{239}Pu [10]. The near-to-magic fragments produced more abundantly with n+^{239}Pu are characterized by low level densities, and higher temperatures [44], as compared to the fragments produced in ^{252}Cf. As a consequence, the PFGS is harder for n+^{239}Pu. The fact that the hardness of the PFGS of fast-neutron induced fission of ^{238}U is finally similar to the one of ^{252}Cf (in experiment like in the calculations), see Fig. 3, is explained by the intense S1 mode in ^{239}U vs. ^{252}Cf fission, which somehow counterbalances the expectation based on S_n alone.

A substantial excess of γ-ray yield between $E_\gamma = 4$ and 8 MeV was observed several decades ago in spontaneous fission of ^{252}Cf with the Crystal Ball NaI array, see Refs. [53,54]

and therein. Thanks to the availability of mass selection, this so-called "γ bump" was assigned to the emission properties of post-neutron fragments in the vicinity of ^{132}Sn. Further measurements did not pay much attention to this, due to the experimental difficulty of extending the spectrum to high E_γ values with sufficient statistics. The advent of new, efficient scintillators leads to a renewed interest in the γ bump. Very recently, the PFGS extracted by Makii et al. [55] in the commissioning of their new $LaBr_3$ detectors seem to confirm the occurrence of such an excess of yield also for thermal-neutron-induced fission of ^{235}U. Though, the work shows at the same time that the reliable extraction of the γ bump requires a very careful analysis, since in the inclusive spectrum, i.e. in the absence of mass gating, its signal remains small (see also Fig. 1a, b in Ref. [56]).

Although the experiments of Qi et al. [19,20] in its present implementation cannot be used to address the origin of the γ bump, due to absence of mass selectivity and low statistics in the corresponding energy region, we propose to discuss the predictions of the calculations in this context. The upper panel of Fig. 7 shows the mass distribution of the post-neutron fragments calculated with FREYA contributing to different slices of the PFGS, between $E_\gamma = 3$ and 6 MeV, for fast-neutron induced fission of ^{238}U. It is predicted that the contribution of heavy fragments with masses around $A = 130$–134 clearly dominates from $E_\gamma = 4$ MeV on. That is, the PFGS for near-to-closed-shell nuclei is harder. A similar result is predicted by FREYA for the other two systems. Calculations by the GEF code, reported in Fig. 122 of Ref. [10], show the same pattern. While the excess of yield measured at Crystal Ball is supported by the calculations to be due to fragments close to ^{132}Sn, contrary to experimental findings, FREYA and GEF do not exhibit a bump-shaped excess; the calculated spectra are simply harder. One cannot exclude that the calculations miss some specific (possibly exotic) γ strength for the involved nuclei. On the other hand, calculations with the FIFRELIN code [3] predicts a PFGS whose shape resembles more a bump (see Fig. 5.14 in Ref. [57]). As compared to FREYA and GEF, the FIFRELIN code models neutron and γ-ray emission within the Hauser-Feshbach theory, and the implementation of RIPL3 discrete levels is slightly different from FREYA. Finding the very origin of the γ bump is therefore expected to benefit from calculations of this kind as for guidance.

Recent measurements [58] at the LANSCE facility with the DANCE array permitted to compare the PFGS in slow-neutron (from about thermal to 100 keV) induced fission of ^{235}U, ^{239}Pu, and ^{241}Pu, as well as the ^{252}Cf standard. The occurrence of various "bumps" from $E_\gamma \approx 0.5$ MeV on, and their dependence on fissioning system above $E_\gamma \approx 5$ MeV, was revealed. It was suggested that the difference in PFGS between the available systems is to be linked to different level-density and dipole resonance properties of the

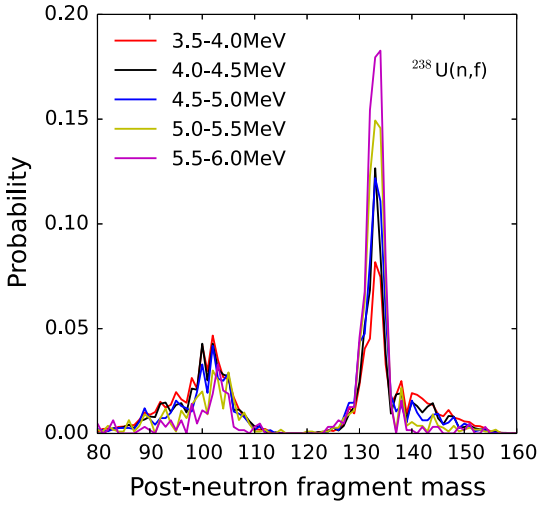

Fig. 7 Post-neutron fragment mass as obtained with FREYA for n+^{238}U and populating specific region of the PFGS, i.e. with $E_\gamma \in$ [3.5–4] (red), [4–4.5] (black), [4.5–5] (blue), [5–5.5] (green), [5.5–6] (violet) MeV. The distributions are normalized to unity for evidencing the relative contribution of the light and heavy fragments depending on the E_γ slice

corresponding fragment population. Unfortunately, the limited resolution of the BaF_2 scintillators prevented the aforementioned interpretation from being further probed, and presumably supported, by differences in the low-energy structure pattern. In addition, no realistic fission-fragment de-excitation calculation was done to deepen the understanding of the observed differences. Like in the present campaign, no mass selection was available. Nevertheless, the outcome clearly demonstrates the significance in pushing such kind of measurements further.

It has finally to be mentioned that the discussion of the γ bump(s) is probably to be linked with the observation made above about the hardness of the PFGS depending on the reaction system. Clearly, dedicated experiments, with efficient set-ups, some level of mass identification, and involving different fissioning systems, are highly desirable to reach a consistent picture. This seems to be possible in reasonably close future [17,55], with straightforward extension [17] of existing set-ups.

4.3 Angular momentum influence

Since γ-ray emission is by far the main mechanism for exhausting angular momentum, it is the observable of choice to trace back the angular momentum generated at scission. The latter, and even more important, the mechanism which is responsible for creating it and partitioning it between the fragments, remains until today a longstanding controversial question (see section III.I in Ref. [10]. Here, we propose a

discussion on the possible evidence of sensitivity to angular momentum.

When measuring γ rays, various methods can be used to extract information on angular momentum, among which photon angular distributions and isomeric ratios. Though, the most direct, model-independent way is certainly to identify the excited states populated in the fragments in order to determine the maximum spin value reached. Since the spin straightforwardly impacts the number of γ rays emitted along the descent of the yrast line, M_γ is a good signature for estimating the maximum angular momentum reached, too. It is thus the low-energy region which is the most useful part of the PFGS, since it concentrates most of M_γ.

Our calculations with GEF predict that the spin acquired by the fragment at scission increase from about 2–7 $\hbar$ over the fragment mass range $A = 80-160$, given at first order by the moment of inertia, and thus also deformation. The slope of the increase slightly depends on the fissioning system. The calculations by FREYA give a similar result, with, though, a somehow smaller average value, around 3–4$\hbar$ and a weaker system-dependence. Inspection of Table 1 led us to conclude that, within the current experimental status and uncertainties, as well as the accuracy of (still other) model assumptions, FREYA and GEF give on average a good description of M_γ. That is, overall the predicted angular momentum looks reasonable, and current M_γ data cannot pretend being sensitive to the difference of a couple of $\hbar$ between the two codes. Regarding the PFGS observable, this difference reflects into different intensities for the characteristic γ-ray transitions. Within the experimental limitations in measuring the low-energy portion of the PFGS discussed above, and the influence of model assumptions, any more precise conclusion regarding the value of L would be highly speculative. Further investigation shows that the major difference between the FREYA and GEF results is in the dependence of M_γ on fragment mass [18]. The difference is strongly related to the treatment of the emission of statistical γ rays, and namely to the amount of spin carried away by the latter. Unfortunately, experimental information about the dependence of M_γ on mass is very scarce, highly model-dependent and still very controversial (see section IX.F. in Ref. [10]).

Regarding the possible evidence of angular momentum effects, we are therefore forced to conclude that the present implementation of the experimental approach is not sensitive to angular momentum within a couple to several $\hbar$. The recent study by Rose et al. [59] suggests that, for an inclusive measurement like here to be sensitive to angular momentum, the L's involved need to span over 3–4 $\hbar$. Model calculations by Litaize et al. [46] suggest that the high-energy part of the PFGS can be sensitive to L at the level of 5 $\hbar$ or so. The recent calculations by Chyzh et al. [50] suggest higher sensitivity. Experimental efforts into the direction of reliable L extraction are definitively needed to settle this point.

Again, we mention that a step beyond the present limitation can be made with a little variant of the set-up [17], giving access to fragment mass within a few units. In the 1960's, Bowman et al. [47] observed that, already with NaI scintillators, fragment spins for most intense channels may be inferred. High-resolution spectroscopy by means of Ge detectors (e.g. Refs. [42,43]) is, of course, best suited to pin down the maximum L populated. Though, lower efficiency in that case hampers the determination of M_γ, which is an important quantity, too. Hence, scintillation- and Ge-detector based experiments are fully complementary approaches.

5 Conclusions and perspectives

Prompt γ-ray spectra emitted in fast-neutron induced fission of ^{239}Pu are presented. A detailed analysis of the low and high energy portions of the spectra, together with fast-neutron induced fission of ^{238}U and spontaneous fission of ^{252}Cf, is performed. The consistency of the data set, collected under similar conditions, permits a robust comparison between the three fissioning systems. The latter is proposed to be guided by calculations using the FREYA and GEF semi-empirical models. Differences in the low-E_γ structures between the various systems point to the possibility of evidencing the influence of fragment population, which is intimately correlated with neutron evaporation. Similarly, comparison in the high-energy region of the E_γ spectra is informative about the fragment properties.

According to the renewal and growing interest of γ-ray emission in fission, the development of more and more elaborate devices and analysis tools, on the experimental side, and the wide popularity of codes which are used for various purposes, on the theoretical side, the present investigation makes a point about the robustness and possibility to address certain physics questions with certain data and models. It sheds light on the influence of the limitations of current methods, as well as it points the potential of the latter when supplemented with the little required development.

To exploit and push further the exploitation to nuclear structure studies and the investigation of energy sharing and angular momentum generation in fission needs mass selectivity. It requires the implementation of position-sens-itive ionization chambers, conserving the 4π efficiency, in conjunction with the high-efficiency PARIS array, both available at the high-intensity fast-neutron beam ALTO/LICORNE. Also the wider mapping of PFGS properties in the actinide region should be performed. Such data will permit to put more stringent constraints on fission models and understanding. Altogether will also constitute valuable input for nuclear applications as set out by the OECD/NEA.

Acknowledgements We thank the staff at the ALTO facility for the production of high intensity beams, and smooth running, as well as we acknowledge support from the PARIS collaboration all along the campaign. We thank J. Randrup and K.-H. Schmidt for enlighting discussions about FREYA and GEF, respectively. We are also very thankful to K.-H. Schmidt for critical reading of the manuscript. We acknowledge funding from the ENSAR2 and CHANDA (Project 605203) programmes of the European Commission. This work was also supported by ELI-NP – Phase II, co-financed by the European Regional Development Fund through programme COP ID 1334.

Data Availability Statement This manuscript has no associated data or the data will not be deposited. [Authors' comment: Data are available from the authors upon request.]

References

1. A.N. Andreyev, K. Nishio, K.-H. Schmidt, Rep. Progr. Phys. **81**, 016301 (2018)
2. K.-H. Schmidt, B. Jurado, Rep. Progr. Phys. **81**, 106301 (2018)
3. O. Litaize, O. Serot, Phys. Rev. C **82**, 054616 (2010)
4. S. Lemaire et al., Phys. Rev. C **72**, 024601 (2005)
5. P. Talou et al., Phys. Rev. C **83**, 064612 (2011)
6. B. Becker et al., Phys. Rev. C **87**, 014617 (2013)
7. R. Vogt et al., Phys. Rev. C **85**, 024608 (2012)
8. R. Vogt et al., Phys. Rev. C **87**, 044602 (2013)
9. O. Litaize et al., Eur. Phys. J. Web. Conf. **169**, 00012 (2018)
10. K.-H. Schmidt et al., Nucl. Data Sheets **131**, 107 (2016)
11. P. Talou et al., Eur. Phys. J. A **54**, 9 (2018)
12. http://www.oecd-nea.org/dbdata/hprl
13. A. Oberstedt et al., Phys. Rev. C **87**, 051602(R) (2013)
14. S. Oberstedt et al., Phys. Rev. C **90**, 024618 (2014)
15. M. Lebois et al., Phys. Rev. C **92**, 034618 (2015)
16. A. Gatera et al., Phys. Rev. C **95**, 064609 (2017)
17. S. Oberstedt et al., Eur. Phys. J. A **51**, 178 (2015)
18. L. Qi, Measurements of prompt γ rays emitted in fission of ^{238}U and ^{239}Pu induced by fast neutrons from the LICORNE neutron source. PhD Thesis, Universite de Paris-Saclay, Paris-Sud (2018). Available at http://www.theses.fr/
19. Liqiang Qi et al., Phys. Rev. C **98**, 014612 (2018)
20. Liqiang Qi et al., Eur. Phys. J. Web. Conf. **169**, 00018 (2018)
21. M. Lebois et al., Nucl. Instr. Methods. Phys. Res. A **735**, 145 (2014)
22. A. Maj et al., Acta Pol. **40**, 565 (2009)
23. R. Billnert et al., Phys. Rev. C **87**, 024601 (2013)
24. A. Chyzh et al., Phys. Rev. C **85**, 021601(R) (2012)
25. A. Chyzh et al., Phys. Rev. C **90**, 014602 (2014)
26. A. Oberstedt et al., Phys. Rev. C **92**, 014618 (2015)
27. A.R. Junghans et al., Phys. Lett. B **670**, 200 (2008)
28. N. Schunck, L.M. Robledo, Rep. Progr. Phys. **79**, 116301 (2016)
29. R. Vogt, J. Randrup, Phys. Rev. C **96**, 064620 (2017)
30. A. Tudora et al., Ann. Nucl. Energy **35**, 1 (2008)
31. FREYA user manual, p. 8–9. https://nuclear.llnl.gov/simulation
32. https://mars.fnal.gov/
33. T. Goorley et al., Initial MCNP6 release overview. MCNP6 version 0.1. Nucl. Technol. **180**, 298 (2012)
34. A. Fasso et al., CERN-2005-10, INFN-TC 05-11, SLAC-R-773
35. C. Schmitt et al., Phys. Rev. C **98**, 044605 (2018)
36. P. Talou et al., Nucl. Data Sheets **118**, 227 (2014)
37. R. Capote, Nucl. Data Sheets **131**, 1 (2016)
38. T. Wang et al., Phys. Rev. C **93**, 014606 (2016)
39. P. Talou et al., Phys. Rev. C **94**, 064613 (2016)
40. G.M. Ter-Akopian et al., Phys. Rev. C **55**, 1146 (1997)
41. R.P. Schmitt et al., Nucl. Phys. A **427**, 614 (1984)
42. A. Bogachev et al., Eur. Phys. J. A **34**, 23 (2007)
43. J. Wilson et al., Phys. Rev. Lett. **118**, 222501 (2017)
44. K.-H. Schmidt, B. Jurado, Phys. Rev. Lett. **104**, 212501 (2010)
45. P. Talou et al., Phys. Proc. **59**, 83 (2014)
46. O. Litaize et al., Eur. Phys. J. Web. Conf. **116**, 10003 (2016)
47. H.R. Bowman et al., Phys. Rev. Lett. **12**, 195 (1964)
48. H. van der Ploeg et al., Phys. Rev. C **52**, 1915 (1995)
49. D. Regnier et al., Phys. Proc. **31**, 29 (2012)
50. A. Chzyzh et al., Phys. Lett. B **782**, 652 (2018)
51. M. Ciemala et al., Phys. Rev. C **91**, 054313 (2015)
52. http://www.nndc.bnl.gov/nudat2/
53. A. Hotzel et al., Z. Phys. A **356**, 299 (1996)
54. P. Singer et al., Z. Phys. A **359**, 41 (1997)
55. H. Makii et al., Nucl. Inst. Methods Phys. Res. A **906**, 88 (2018)
56. J.B. Fitzgerald et al., Z. Phys. A **355**, 401 (1996)
57. D. Regnier, Contribution a l'etude des γ prompts de fission. PhD thesis, University Grenoble, France (2013)
58. A. Chyzh et al., Phys. Rev. C **87**, 034620 (2013)
59. S.J. Rose et al., Phys. Rev. C **96**, 014601 (2017)